Contents lists available at ScienceDirect

Solar Energy Materials and Solar Cells

Suitability and characteristics of rocks for sensible heat storage in CSP plants

R. Tiskatine[a,*], R. Oaddi[a,b], R. Ait El Cadi[a,b], A. Bazgaou[a], L. Bouirden[a], A. Aharoune[a], A. Ihlal[b]

[a] Thermodynamics and Energetics Laboratory, Faculty of Science, IbnZohr University, BP8106, 80006 Agadir, Morocco
[b] Materials and Renewable Energies Laboratory, Faculty of Science, IbnZohr University, BP8106, 80006 Agadir, Morocco

ARTICLE INFO

ABSTRACT

High temperature thermal energy storage (TES) is a crucial technology ensuring continuous generation of power from solar energy and plays a major role in the industrial field. Choosing the optimal storage material remains a great challenge. From the literature, it is understood that the natural rock is a good suitable material for TES in concentrating solar power (CSP) plants. However, not much work has been published on the behavior of rock and its suitability for TES. This paper evaluates the potential of rocks as candidate materials for use in high temperature thermal storage. On one hand, we provide literatures on sensible heat storage (SHS) materials and works carried out on packed rock beds, and on the other hand, experimental tests are conducted and data are analyzed and discussed in order to choose the best rocks among fifty two varieties. According to various criteria, the obtained results show that dolerite, granodiorite, hornfels, gabbro and quartzitic sandstone are the good candidates to be used as storage materials for air-based solar systems.

1. Introduction

Renewable energies have nowadays attracted more attention due to the shortage of fossil fuels and their polluting emissions. Solar energy is the most extensively available of all the renewable energy resources. However, it is intermittent and unavailable every time. Thermal energy storage (TES) is considered as a promising technology to exploit renewable energy [1–3] and an effective way to get the supply of energy at all times and to regulate the mismatch between energy generation and energy demand. It plays a very important role in optimizing concentrated solar power (CSP) technology [4]. The latter was considered as one of the most optimal and flexible technologies to produce electricity from renewable energy [5]. Moreover, TES improves the performance of energy systems.

TES can be stored in the form of sensible, latent or chemical heat storage [2,6]. It can also be stored by combinations of sensible and latent heat storage [7]. Sensible heat storage (SHS) systems store energy by heating a storage material without changing the phase, while the latent heat storage (LHS) involves a phase transition (melting and solidification) of a phase change material (PCM). Chemical heat storage is associated with reversible chemical reaction.

A number of studies and reviews concerning the TES technologies are available in the literature. Hasnain [8] reviewed several TES technologies and compared SHS and LHS. Ismail and Stuginsky [9] compared various numerical models for TES in packed bed, both for SHS and LHS. Zalba et al. [10] reviewed TES systems based on PCMs.

Kenisarin et al. [11] give an extensive summary of high temperature LHS materials. Gil et al. [12] reviewed and classified different TES concepts. A comparable work to that of Zalba et al. [10] was reviewed by Oró et al. [13] for cold TES applications. Cot-Gores et al. [14] reviewed the experimental research on thermo-chemical energy storage. They pointed out that the low thermodynamic efficiency of the basic cycle is among the drawbacks in solid–gas chemical reactions. An extensive review of the various TES systems and technologies applicable to CSP plants was published by Kuravi et al. [15]. Zanganeh et al. [16] proposed the combination of SHS and LHS for stabilizing the outflow air temperature of a packed bed of rocks during discharging. Same approach was used recently by Geissbuhler et al. [4].

LHS has a higher storage density compared to the SHS [1,17,18], however, the PCMs are expensive, requires a complex geometry [19] and have short lifetime. Furthermore, the majority of PCMs have low thermal conductivity [17,20,21], which slows down the heat transfer rates during charging and discharging process leading to complex heat exchanger systems. This problem has led to a number of studies for improving heat transfer. Among these studies, Almsater et al. [21] used axially finned heat pipes, Peiro et al. [22] used multiple PCMs configuration instead of the single PCM, Zhao et al. [23] and Sobolciak et al. [24] used paraffin and expanded graphite and Huang et al. [20] used metal fins with high thermal conductivity to increase heat transfer surface areas. A review on the most techniques used is conducted by Gasia et al. [25] and Agyenim et al. [26]. The main drawback of these techniques is associated to the increase of costs and the corrosion

problems. On the other hand, the organic PCMs are flammable [10] and require temperatures below 150 °C [27], whereas, the inorganic PCMs are corrosive [28]. The metallic PCMs have high thermal conductivity, however, because of the very high cost, the use of these materials in thermal storage is not very widespread.

According to Singh et al. [29], the technological and economical aspects make SHS superior than LHS. Compared to the other storage methods, it is the most common technology [30] that is simple in design and operation, inexpensive and most economic in TES system [18,31,32]. It can be used in a wide temperature range. Furthermore, SHS materials are inexpensive and have larger thermal conductivities when compared with most of PCMs used [7].

Several materials have been used in SHS applications. Molten salts are the most widely researched and used in CSP plants. Water is the most used for low temperatures applications (between 25 and 90 °C) [8]. In term of cost, rocks, sand and soil are the most popular storage materials selected in several projects. A review of materials used in high temperature TES applications was given by Gil et al. [12]. On the other hand, Duffie and Beckmann [33], Singh et al. [29] and Dinker et al. [18] presented different materials suitable for TES.

This present work evaluates the potential of fifty two varieties of rocks to be used as high temperature storage materials. The main objectives of the paper are: (1) to review the properties of SHS materials considered in literature and works reported on packed rock beds; (2) to provide experimental data of various rock types; and (3) to test and interpret the measured characteristics in order to select the best suitable rocks for high temperature TES.

2. Literature review

This section provides a brief overview on the properties of SHS materials found in literature and previous works on rock bed thermal storage.

2.1. Sensible heat storage materials

SHS materials characteristics have been studied in several applications over the last decades. SHS consists in increasing the temperature of a storage material (solid or liquid). Molten salt, water, oil, steam, stone, brick and concrete are the most common storage materials used in TES systems and are commercially available. Ataer [34] stated that the choice of a storage material depends mostly on the temperature level of the required application.

For sensible TES materials, the most desirable characteristics are high energy density, good thermal conductivity, chemical stability and high resistance to thermal cycling damage, environmentally friendly and low CO_2 emission, high availability and low cost, low thermal expansion and little variation in the volume, long time service with a wide temperature range and easy use. Other desirable characteristics are good heat transfer between storage material and heat transfer fluid (HTF) and its compatibility with the container material [1,3,12,35–37].

Tables 1, 2 present, respectively, the most important properties from literature for a number of different rock types and for different other sensible storage materials.

From the data collected in Tables 1, 2, we can observe that some properties of rocks are similar to those of other heat storage materials. It can also be seen that rocks have good storage capacity. The variation of thermal properties between rocks is due to the proportion of minerals and impurities existing in the rock, the different geological ages of rocks and the difference in place of origin [56]. The tests carried out by Xu et al. [61] on five storage materials including quartzite rock, silicon carbide ceramic, high temperature concrete, cast iron and alumina ceramic showed that the five materials have about the same effective discharge efficiency.

Taking into account the combination of the requirements of a TES system, rocks can be considered as feasible solution. They are abundant and freely available in many areas, economical and requires only transport to the site, thermally and chemically stable in a wide temperature range, non-toxic and non-flammable. They have high specific heat, good thermal conductivity, very low thermal expansion coefficient and high mechanical resistance to thermal cycling (the melting point of all rocks exceeds 900 °C). Moreover, rocks act both as heat transfer surface and storage medium and does not require an expensive HTF. Their processing is easy and the heat transfer is good when used with air [7,29,83,114–118].

The choice of HTF is also an important component of TES systems.

Table 1
Thermo-physical properties from literature of certain rock types.

Rock	Density (g/cm^3)	Thermal conductivity at 20 °C (W/m. K)	Specific heat at 20 °C (J/Kg.k)	Thermal capacity (kJ/m^{3}K)	Uniaxial compressive strength (MPa)	References
Granite	2.6–2.7	2,6–3.1	600–950	1560–2517	100–350	[29,34,38–52]
Limestone	2.3–2.8	2.0–3.0	683–908	1584–2506	30–250	[34,38–41,44,46,49,53–59]
Marble	2.6–2.7	2.3–3.2	800–883	2080–2366	50–200	[34,38–40,43,46,49,50,57]
Quartzite	2.5–2.6	2.9–5.7	623–830	1557–2191	150–300	[38,40,43,44,46,48,49,51,52,54,55,57,60–62]
Sandstone	2.2–2.6	1.7–2.9	694–950	1492–2508	20–260	[34,38–40,44,46,48,49,53,57,58,63–66]
Granodiorite	2.7	2.1–2.6	650–1020	1735–2784	252	[39–42,44,51,52,67]
Gabbro	2.9–3.0	1.5–2.6	600–1000	1722–3030	150–350	[39–42,45,46,48,50,51,55–57,68–70]
Basalt	2.3–3.0	1.2–2.3	700–1230	1603–3714	67–400	[39,40,43,44,46,48,49,51,56,63,68,71]
Hornfels	2.7	1.5–3.0	820	2246	100–533	[40,43,48,72]
Schist	2.6–2.8	2.1–3.0	790–1100	2085–3080	60–400	[39,40,44,51,52]
Quartzitic sandstone	2.6–2.6	5.0–5.2	652	1714–1721	120	[48,50,73]
Rhyolite	2.3–2.6	1.6–2.3	785	1805–2041	120–250	[40,48,49,73–75]
Andesite	2.6–2.7	2.3–2.8	815	2127–2167	183–400	[39,40,51,66]
Calcareous sandstone	2.7	4.4	652	1734	0.1–15.8	[55,76]
Steatite	2.7–3.0	2.5	980–1068	2626–3182	10.1	[77,78]
Dolerite	2.7–2.9	2.2–3.0	870–900	2305–2610	100–350	[39,44,51,57,79]
Slag	2.7	0.6	840	2268	–	[80]
Gneiss	2.7	2.7–3.1	770–979	2080–2640	48–300	[40,51,81,82,86]
Clay	1.5–2.3	0.7–1.5	860–880	1320–1830	–	[28,51,83]
Schale	2.8	1.1–2.1	820 (45 °C)	2255 (45 °C)	34–75	[40,58,79,84,85]
Diorite	2.8–3.0	2.5	1000	2800–3000	170–300	[40,51,86]
Argillite	2.3–2.6	2.1–2.3	838	1927–2136		[51,53]
Dolomite	2.8	2.1	802	2205–2269	150–170	[40,53,87]

Table 2
The main characteristics from literature of the most common sensible thermal storage materials.

Material	Characteristics					Disadvantages
	Density (g/cm³)	Thermal conductivity at 20 °C (W/m K)	Specific heat at 20 °C (J/kg K)	Thermal capacity (kJ/m³K)	References	
Concrete	2.2–2.7	0.9–2.0	750–1130	1680–3005	[8,29,38,46,88,89]	1. Decrease of compressive strength at 400 °C [12] 2. Decomposition at about 450 °C [2] 3. - Low tensile strength [102]
HT concrete	2.8	1.0	916	2519	[61,90]	1. - Low thermal conductivity
High alumina concrete	2.4	0.2	980	2352	[2,91]	1. - High volumetric expansion [2] and low thermal conductivity
Reinforced concrete	2.2	1.5	850	1870	[12]	1. - High form cost [102] 2. - Difficulty of machining
Cement mortar	1.9–2.0	0.6–0.7	642	1194–1309	[92,93]	1. - Low thermal conductivity and energy density
Castable ceramic	3.5	1.4	866	3031	[12,27]	1. - High investment cost [103] 2. - Deterioration at high temperature (> 400 °C) [27]
Alumina ceramics	3.8–4.0	18.0–33.0	755–880	2831–3484	[31,61,94,95]	1. - Long time and high cost of production
Silicon carbide ceramics	3.2	120.0	750	2407	[61]	1. - Higher cost and long process times [104] 2. - Limited thermal shock resistance [74]
Brick	1.7–1.8	0.5–0.7	840	1419–1512	[8,80]	1. - Low thermal conductivity and energy density
Brick magnesia	3.0	5.0–5.1	1130–1150	3390–3450	[12,29]	1. - Low resistance to thermal shock [105]
Silica fire bricks	1.8	1.5	1000	1820	[12]	1. - Low strength [106]
Soil (clay)	1.5	1.3	880	1276	[80]	1. - Low energy density
Soil (dry)	1.3	0.3	795	1001	[8]	1. - Low thermal conductivity
Soil with gravel	2.0	0.5	1840	3680	[28]	1. - Low thermal conductivity
Silica-based refractory	2.3	1.8	863	2019	[80]	1. - Higher cost
Copper	8.3–9.0	372.0–385.0	383–419	3178–3729	[8,29,80]	1. - Higher thermal expansion and cost [18]
Iron-Cast iron	7.2–7.9	29.3–73.0	465–837	3348–6612	[8,13,61,80]	1. - Higher thermal expansion, high cost [107] and high weight [18]
Aluminum	2.7	204.0–238.4	896–945	2419–2551	[77,80]	1. - Higher thermal expansion [18]
Lead	11.3	35.3	131	1485	[96]	1. - High cost [18] and low thermal capacity.
Steel- Cast steel	7.8	40.0–50.0	571–600	4453–4680	[12,77]	1. - High thermal expansion, high weight [18] and high cost
Steel Slag	3.0	2.0–3.5	996	2968	[62]	1. - Higher cost [62,108]
Cofalit	3.1	1.4–2.7	800–1034	2496–3226	[6,97]	1. - Long time of production (cost)
Graphite	2.2–2.3	122.0–155.0	401–610	882–1378	[80,98]	1. - Oxidation into CO2 in contact with air at high temperature [98]
Soda-lime glass	2.7	0.9	703	1905	[98]	1. - Low thermal conductivity
Sodium chloride	2.2	6.5–7.0	850–860	1836–1861	[12,80]	1. - High thermal expansion coefficient and decrease of density with temperature [109]
Molten salts	0.5–2.6	0.2–2.0	1500	1350–3900	[6,99,100]	1. - Low thermal conductivity [110] 2. - Need of complex equipment [5,111] 3. - Higher cost and high freezing point [12,15,112]
Solar salt	1.9	0.5	1495	2825	[62]	1. - Low thermal conductivity
Mineral oil	0.8	0.1	2600	2002	[100,101]	1. - Low thermal conductivity 2. - Expensive and environmentally unfriendly
Synthetic oil	0.9	0.1	2100–2300	1890–2070	[12,100,101]	1. - Low thermal conductivity 2. - High costs and limited life [36] 3. - Not environmentally friendly [36,79] 4. - Degradation at high temperature (> 400 °C) [113]
Liquid sodium	0.9	71.0	1300	1105	[12]	1. - High vapor pressure (dangerousness)
Water	1.0	0.6	4187	4174	[45]	1. - Limited temperature and low thermal conductivity [19] 2. - High vapor pressure [18] and corrosiveness

Gil et al. [12] studied different HTFs used for high temperature TES. The typical HTF used are air, thermal oil, molten salt and water. Water has high vapor pressure and corrosiveness. The majority of thermal oils are costly, hazardous, limited in their temperature range and have high vapor pressure which is lower than water. In this case, it was necessary to use adequate infrastructure [62,119]. Molten salts are very corrosive and their thermal conductivity is low. Moreover, they have melting points above 200 °C which limits the extraction of the stored heat. In this case, a temperature maintenance during the night when solar energy is not available could lead to a high consumption of energy.

Comparing the HTFs used, air is the most abundant, cheaper and easily available everywhere. It is inflammable, non-toxic, non-degradable and more environmentally friendly. It can operate at low and high temperature. According to Coutier and Faber [120], the most suitable system to store heat utilizes air as HTF. In addition, with air the storage operation is simple.

2.2. Packed rock bed thermal storage

Rock bed using air as HTF became one of the most optimal solutions
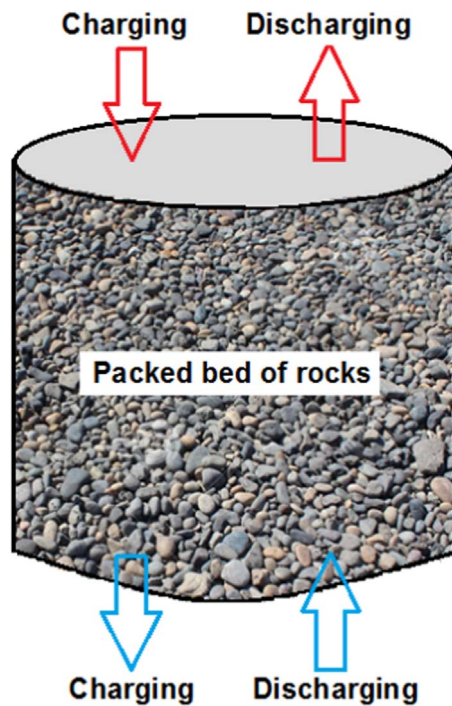
Fig. 1. Schematic of a packed rock bed storage unit with operating principle.

for thermal storage in solar power plants because it offers several advantages such as low investment cost, efficiency, reliability and environmentally friendliness [29,79,114,121–123]. It is well suited for CSP plants since it is a simple technique allowing high overall thermal efficiency [29,36,55,77,114,120,123]. According to Heller and Gauché [122] and Barton et al. [117], it does not need an additional heat exchanger between the collector and the heat tank.

A schematic of a packed rock bed storage unit is shown in Fig. 1. During the charge phase, the hot fluid received from solar collectors enters through the top of bed (downward) and transfers heat to the rocks. During the discharge phase, when energy is needed, the low temperature fluid circulates in the opposite direction (from the bottom) and heated by the rocks. Charging from the top allows maintaining of thermal stratification in the bed [114]. Packed bed is generally well insulated to avoid the heat losses. According to Okello et al. [7], the total energy stored in a bed containing only rocks from initial average temperature T_i to final average temperature T_f is given by

$$E_{rocks} = \rho_r C_{p,r} (1 - \varepsilon) V (T_f - T_i) \tag{1}$$

where E_{rocks} is the energy stored in Joule, ρ_r is the density of rock in kg/m^3, $C_{p,r}$ is the specific heat capacity of rock in J/kg.K, ε is the void fraction without unit and V is the total volume of the storage container in m^3. T_i and T_f are in Kelvin.

There is several works reported on various aspects of packed bed thermal storage including experimental tests and modeling with a particular interest devoted to the rock bed with air as HTF that is deployed in several CSP power plants. Among these works, only a few have studied the thermophysical properties, the mechanical behavior at elevated temperatures and the thermal cycling resistance of the rocks. Furthermore, limited knowledge exists on the relevant properties of rocks used as medium of storage. In 1980, Curto and Stern [124] proposed a solar power of electricity production based on a packed bed of slag rock heated by air at approximately 540 °C to store about 5000 MWh$_{th}$. They pointed out that slag is thermally and mechanically stable in structure up to 1200 °C. However, Allen [79] thermally cycled slag samples between 30 °C and 510 °C and found that they all broke apart within 60 cycles. In 1982, Coutier and Farber [120] presented a numerical model and conducted experiments to describe the heat

transfer process within a rock bed using air as working fluid. They measured the thermal properties of different rock types. The thermal conductivity of rocks used is very low (about 0.48 W/m K), which is a drawback for a thermal storage system. In 1984, Beasley and Clark [125] compared experimental data of a packed rock bed thermal storage with a developed two-dimensional numerical model. Air was used as HTF in their study. In 1990, Ammar and Ghoneim [83] presented a thermal storage unit packed with spheres of clay (natural rock) and based on solar-air heating systems. They optimized the parameters of the bed by the aid of a developed computer program. The thermal conductivity indicated in this study (about 0.72 W/m K) is also low for a storage material. In 1991, Meier et al. [123] developed a mathematical model describing the thermal behavior of a packed bed of rocks with high temperature air as HTF (up to 700 °C), and built an experimental container to validate this model. In the same year, Fricker [118] discussed the suitability of five varieties of rocks for thermal storage and showed the great potential of using rock beds at high temperature. The rocks studied were thermally cycled between 20 and 600 °C and the limestones are among those that desintegrated. In 1991 also, Sagara and Nakahara [126] developed a theoretical model of the heat transfer process within a packed bed of gravel with air as heat transfer medium. In 2002, Pacheco et al. [127] developed a pilot scale thermocline thermal storage system filled with rocks. They showed that quartzite and silica sand are the most suitable storage materials in combination with molten salt used as working fluid. Same result was obtained by Brosseau et al. [112] in 2005 by testing several rock types. Nevertheless, Mills [113] stated that the sand and rock containing the silica caused the oil to degrade when used as HTF.

Recently, some other works have been reported about the numerical investigation and the experimental validation of the rock beds with air as the medium of heat transfer. In 2011, Hänchen et al. [77] analyzed a packed bed of steatite rock for air-based CSP plants at temperature up to 520 °C and developed a heat transfer model for the storage system. They found that the overall efficiency exceeds 90% and the volumetric heat capacity is the most relevant property of the storage material. One year later, Zanganeh et al. [55] studied 6.5 MWh$_{th}$ packed bed of rocks at temperatures up to 650 °C using air as HTF, and described a pilot-scale for use at solar thermal plants. They experimentally measured the thermal properties of the five types of rocks used in the packed bed. Among these rocks there is the limestone that is unsuitable at elevated temperatures [118]. An additional study to that of Hänchen et al. [77] is presented by Barton [117] in 2013. He developed and numerically solved a formulation for one-dimensional flow of air through a packed bed of steatite rock for the case when air exhibits density variations with temperature. The thermophysical properties of this rock are the same as those used by Hänchen et al. [77]. In 2014, Liu et al. [121] studied experimentally the heat storage and heat transfer behavior of compressed air flowing through a rock bed of granite rock at temperature up to 120 °C. They measured experimentally the specific heat capacity in the range of 20–170 °C. In the same year, Okello et al. [7] presented an experimental setup to investigate the thermal behavior of TES system with combination of rock particles and phase change material (PCM) with air as HTF at about 350 °C. They showed that the insertion of PCM into the rock bed increases the energy content of the bed and decreases the thermal stratification and the transient charging efficiencies. With the aim of testing the suitability of rocks for thermal storage, thermal cycling was conducted by Allen et al. [128] between 350 °C and 500–530 °C, at rates of 2 °C/min. The results showed that the dolerite withstood thermal cycling well and can be used in packed bed thermal storage.

Most recently, in 2015, Zavattoni et al. [129] evaluated the thermal stratification of an industrial-scale TES system based on a packed bed of river pebbles (gravel) with 25 m^3 in volume and air as working fluid. They have not provided the thermophysical properties of these rocks. In other work, Singh et al. [115] studied the thermal performance of a packed bed TES system filled with 8500 kg of rock pebbles and air as

HTF. They found that heat retrieval efficiency of this bed was better compared to the packed bed filled with PCM and the heat storage capacity can be increased by using medium-sized rock pebbles (5 cm equivalent diameter). In 2016, Grirate et al. [130] compared the potential of six rocks proposed as storage materials and their compatibility with synthetic oil as HTF. They experimentally measured the thermophysical properties of these rocks in the temperature range between 25 and 300 °C and found that quartzite and cipolin rock are the most suitable filler materials for TES. They stated that, unlike the thermal oil, the air is fully compatible with rocks. The study carried out by Hoffmann [62] on the compatibility of vegetable oils with rocks showed the degradation of the oils with quartzite and slag rock. In other work, Jemmal et al. [81] investigated the potential of two gneiss rocks as storage materials for an operating temperature of 550 °C. They experimentally measured the thermophysical and chemical properties of these rocks. Thermal cycling tests carried out by Allen et al. [128] showed the cracking of gneiss after several thermal cycles. In their article, they summarized the method of formation of most rock types and characteristics susceptible to affect the suitability of rocks for thermal storage.

From the literature, it can be pointed out that rocks are very important in TES systems and can be used for thermal storage at low and elevated temperatures. However, very few studies have been conducted to determine their thermophysical properties and their ability to undergo thermal cycling. The latter is an important factor since a CSP plant is expected to several years. The suitable rock should therefore be selected as carefully as the other components in the storage system. In the next part, the characteristics of the rocks including thermal cycling resistance and thermophysical properties will be studied to select the most suitable rocks for thermal storage.

3. Experimental work

The experimental approach and the selection of the most promising rock samples are presented here.

3.1. Testing rock

Rock samples were taken from various sites in Morocco. They were identified in the Geology Department of Ibn Zohr University. A geological map is presented in Fig. 2 to show the sample locations. It shows that rocks are available in most regions of Morocco. The designation, type and origin of studied rock samples are listed in Table 3.

3.2. Characterization and rock types suited to thermal storage

In order to test the performances of rocks for high temperature TES and to know which rock type is suitable for this application, we determined the thermal cycling resistance and the thermo-physical and mechanical properties of these rocks. These parameters are very important to evaluate the thermal performance and lifetime of the storage unit.

3.2.1. Density, porosity and hardness

In the thermal storage field, physical and mechanical properties of the storage material are important. Rocks need to have sufficiently high compressive strength to avoid crushing at the bottom of the tank by the load of rocks stacked above them. The crushed rocks can block the airflow passage. According to the literature, there are very strong relationships between hardness and compressive strength. Hardness measurement is therefore used to predict the compressive strength of rocks. A high density is desirable to increase the thermal capacity of storage. It can also increase the compressive strength of rock.

Porosity plays a significant role in mechanical properties of rocks. In our previous work [73], we have shown, for rocks that cannot withstand high temperature, that the porosity increases and hardness decreases with repeated thermal cycles. Such diminishment could imply undesirable problems in the storage tank.

Apparent density and particles density are obtained by dividing the weight of the sample by its volume. The mass is measured using an electronic scale (resolution of 0.1 g). After the mass measurement, rock was placed in a vase filled with water to absorb the maximum of water. The latter was removed from the surface and the volume of the rock was measured using a graduated test tube. Porosity was determined by dividing the volume of sample by the volume of pore. The hardness test was carried out using a durometer instrument type FM 700e with a load of 2 kg during ten seconds. The test was conducted by applying an axial load to the sample and measuring the corresponding deformation. Experiments were conducted three times for each sample to ensure the reproducibility of the measurements and the average values were used.

The measured properties for all rock types are summarized in Table 3. Loss on ignition is the mass loss resulting from the heating of the rocks at temperatures of 650 °C. Density and hardness of the samples range, respectively, from 2137 to 2864 kg/m^3 and from 40 to 310.9 HV. The average values of porosity are, respectively, 3.4, 3.26 and 8.4 for igneous, metamorphic and sedimentary rocks. High porosity of sedimentary rocks is due to the fact that grains are not filled during sedimentation.

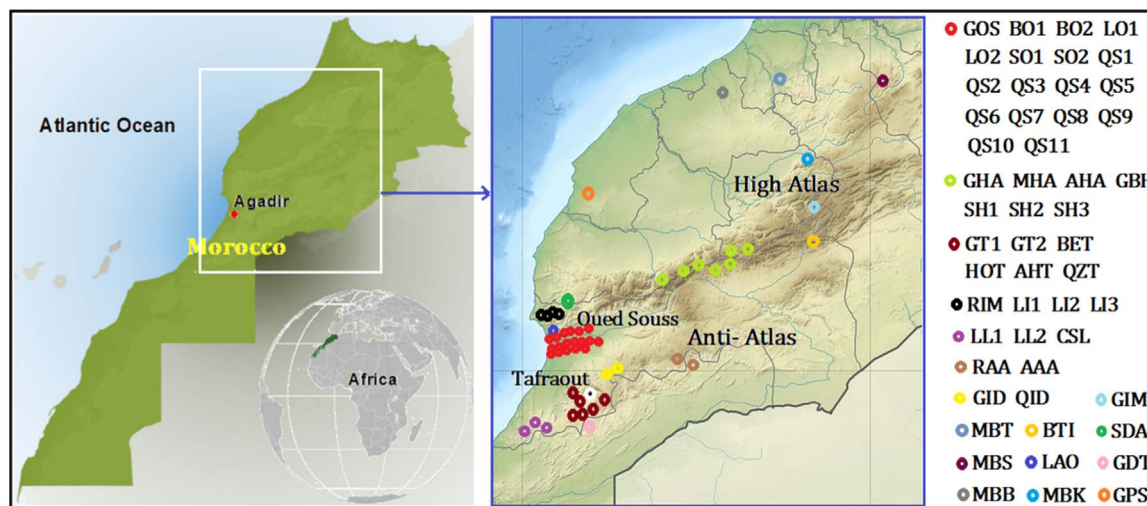The relationship between hardness (HV), density (ρ) and porosity

Fig. 2. Samples location in geological map of Morocco.

Table 3
Designation, origin and measured properties of all studied rocks.

Rock category	Sample	Rock type	Location	Bulk density (g/cm³)	Particle density (g/cm³)	Porosity (%)	Loss on Ignition (%)	Hardness (HV)	State after the last thermal cycle
Igneous	GT1	Granite	Tafraout	2.606	2.659	1.99	0.32	224.5	Disintegration (12)
	GT2	Granite	Tafraout	2.712	2.734	0.80	0.17	255.4	Disintegration (45)
	GHA	Granite	High Atlas	2.725	2.788	2.26	1.18	144.3	Disintegration (8)
	BET	Dolerite	Tafraout	2.715	2.800	3.04	0.73	163.6	Stability (150)
	MHA	Microgranite	High Atlas	2.647	2.737	3.28	1.69	150.1	Fragility (70)
	GOS	Granodiorite	Oued Souss	2.727	2.848	4.25	0.66	171.3	Stability (150)
	GDT	Granodiorite	Tarsouate	2.596	2.728	4.84	0.18	134.3	Cracking (60)
	BO1	Basalt	Oued Souss	2.681	2.845	5.76	0.62	157.6	Stability (150)
	BO2	Basalt	Oued Souss	2.661	2.695	1.26	0.36	114.5	Stability (150)
	BTI	Basalt	Tinghir	2.622	2.852	8.06	1.07	102.7	Stability (150)
	RIM	Rhyolite	ImiMiki	2.640	2.651	0.41	0.52	310.9	Stability (150)
	RAA	Rhyolite	Anti-Atlas	2.601	2.698	3.59	0.18	175.4	Stability (150)
	AAA	Andesite	Anti-Atlas	2.716	2.872	5.43	1.39	123.6	Stability (150)
	AHA	Andesite	High Atlas	2.655	2.851	6.87	1.02	124.9	Stability (150)
	GIM	Gabbro	Imilchil	2.864	2.896	1.10	0.92	210.9	Stability (150)
	GBH	Gabbro	High Atlas	2.664	2.738	2.70	1.46	175.9	Stability (150)
	GID	Gabbro	Ida Ougnidif	2.713	2.776	2.27	2.92	226.5	Stability (150)
Sedimentary	LO1	Limestone	Oued Souss	2.600	2.921	10.99	0.65	71.6	Fragmentation (72)
	LO2	Limestone	Oued Souss	2.578	3.023	14.72	1.69	77.4	White surface (22)
	LAO	Limestone	Agadir Oufella	2.612	2.947	11.37	1.31	82.5	White surface (95)
	LL1	Limestone	Lakhsas	2.652	2.891	8.27	0.04	95.8	Cracking (12)
	LL2	Limestone	Lakhsas	2.675	2.802	4.53	0.10	99.6	White surface (12)
	LI1	Limestone	ImiMiki	2.653	2.875	7.72	0.96	95.2	Cracking (50)
	LI2	Limestone	ImiMiki	2.560	2.840	9.86	3.48	66.4	Fragmentation (2)
	LI3	Limestone	ImiMiki	2.653	2.884	8.01	2.14	106.7	White surface (80)
	SO1	Sandstone	Oued Souss	2.643	2.716	2.69	0.97	156.4	Stability (150)
	SO2	Sandstone	Oued Souss	2.563	2.716	5.63	1.12	158.4	Stability (150)
	SDA	Sandstone	Argana	2.486	2.720	8.60	2.03	40.0	Stability (150)
	CSL	Calcareous sandstone	Lakhsas	2.579	2.784	7.36	0.87	102.8	Cracking (48)
	GPS	Gypsum	Safi	2.137	2.368	9.76	19.2	48	White surface (2)
Metamorphic	HOT	Hornfels	Tafraout	2.667	2.884	7.52	0.68	129.6	Stability (150)
	AHT	Andalusite hornfels	Tafraout	2.594	2.765	6.18	2.11	93.1	Stability (150)
	SH1	Schist	High Atlas	2.698	2.874	6.12	0.77	46.5	Separation (5)
	SH2	Schist	High Atlas	2.659	2.804	5.17	0.49	154.9	Stability (150)
	SH3	Schist	High Atlas	2.591	2.971	12.79	0.80	72.1	Stability (150)
	QZT	Quartzite	Tafraout	2.650	2.698	1.78	0.06	185.9	Stability (150)
	QID	Quartzite	Ida Ougnidif	2.600	2.627	1.03	0.24	252.7	Stability (150)
	MBK	Marble	Khénifra	2.614	2.717	3.79	0.72	110.1	White surface (38)
	MBT	Marble	Tiflet	2.653	2.720	2.46	0.39	128.9	Cracking (30)
	MBB	Marble	Benslimane	2.678	2.759	2.93	0.27	137.7	Cracking (32)
	MBS	Marble	Sefrou	2.540	2.709	6.24	2.35	149.3	Cracking (28)
	QS1	Quartzitic sandstone	Oued Souss	2.761	2.773	0.43	1.19	183.4	Stability (150)
	QS2	Quartzitic sandstone	Oued Souss	2.746	2.760	0.51	0.71	209.6	Stability (150)
	QS3	Quartzitic sandstone	Oued Souss	2.776	2.787	0.39	0.87	205.3	Stability (150)
	QS4	Quartzitic sandstone	Oued Souss	2.670	2.725	2.02	1.59	162.2	Stability (150)
	QS5	Quartzitic sandstone	Oued Souss	2.690	2.762	2.60	1.98	123.4	Stability (150)
	QS6	Quartzitic sandstone	Oued Souss	2.702	2.736	1.24	1.23	187.3	Stability (150)
	QS7	Quartzitic sandstone	Oued Souss	2.800	2.820	0.71	0.38	241.6	Stability (150)
	QS8	Quartzitic sandstone	Oued Souss	2.698	2.711	0.48	0.87	243.2	Stability (150)
	QS9	Quartzitic sandstone	Oued Souss	2.651	2.700	1.81	1.28	223.2	Stability (150)
	QS10	Quartzitic sandstone	Oued Souss	2.650	2.740	3.28	0.57	113.9	Stability (150)
	QS11	Quartzitic sandstone	Oued Souss	2.605	2.664	2.21	1.04	205.0	Stability (150)

(p) for all tested rocks is shown in Fig. 3. As expected, hardness and density decrease as porosity increases. Logarithmic regression is used to provide the correlation between the three physical properties. The best fit correlation is represented between hardness and porosity with a coefficient of determination $R^2 = 0.674$.

Rock strength is generally greater for fine-grained rocks [131] and those containing quartz as binding material [92,128]. It decreases with increase in porosity [132,133]. In the following, the thermal cycling resistance tests are presented and discussed.
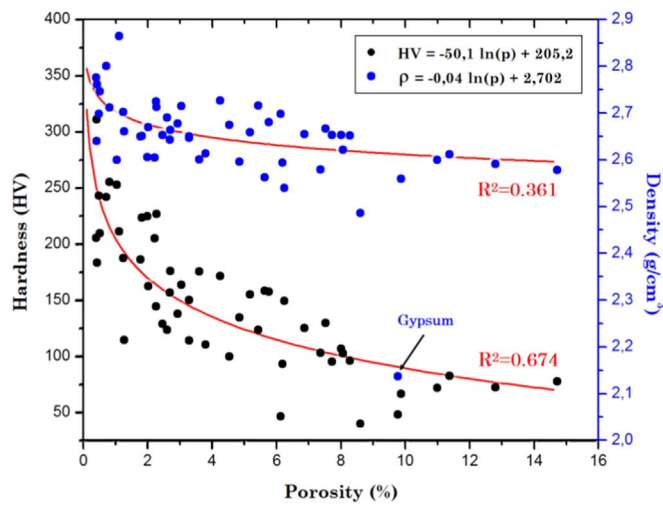
Fig. 3. Relationship between hardness, density and porosity.

3.2.2. Thermal cycling resistance

In order to determine their ability to undergo thermal cycling, the rock samples were thermally cycled between room temperature and 650 °C at rates of 25 °C/min in a heating apparatus (high temperature furnace) and at atmospheric pressure. The specimens were placed in the furnace for approximately 60 min and then cooling in ambient conditions for 40 min at same rates. Fig. 4 shows the shape of studied rock samples. The average equivalent diameter is equal to 4 cm. The choice of higher heating rates reduces the number of cycles performed for each sample. Moreover, after each initial charging and discharging cycle of the bed, the rocks will be suddenly exposed to higher rate of temperature change. In this case, it is possible that microcracks will appear in the first cycles. These microcracks can be expanded during thermal cycling even under normal charging rates (1–2 °C/min).

Infrared images of a rock sample during the charging cycle and the temperature difference between the air in the furnace and the rock sample are shown in Fig. 5. It can be found from these photographs that during the charging period, the sample takes the oven temperature step by step until the temperature difference is zero. It follows from this that rock is compatible with air.

The physical changes in the rock specimens were carefully examined after each thermal cycle. The results are summarized in Table 3. Values in parentheses indicate the number of cycles performed for each sample. Photographs of four important statuses in which one can find rocks after performing the thermal cycling are presented in Fig. 6.

In their report, Zhang et al. [134] discussed the change of physico-mechanical properties of rock after high temperature treatment (up to 500 °C) and showed that this change is related to the dehydroxylation of water and the expansion of solid mineral. Recently, in our paper [73], we discussed the parameters influencing lifetime of rock during

Fig. 4. Shape of rock samples.

thermal cycling and we concluded that the deterioration of rock properties is due to the increases of porosity and microcracks with thermal cycling. This does not always mean that rocks with higher initial porosity are susceptible to degradation with thermal cycling. They sometimes suffer less from fracture compared to the rocks with lower initial porosity.

Disintegration of limestone samples LO1, LL1, LI1 and LI2, calcareous sandstone sample CSL and marble samples MBT, MBB and MBS is due to the decomposition at high temperature of $CaCO_3$ (the main constituent of carbonated rocks) giving CaO and CO_2. Calcium oxide (CaO) appears as a white color on the surface of limestone samples LO2, LAO, LL2 and LI3, marble sample MBK and gypsum sample GPS. The white powder and the poorly bonded particles can block the flow passages and reduce the heat transfer between air and rock in the bed [128]. This means that these rocks are unsuitable for use in high temperature thermal storage.

The cracking of granite samples GT1, GT2 and GHA, microgranite sample MHA and granodiorite sample GDT are formed mostly at the grain boundaries between minerals [135,136]. The phenomenon is attributed to the increase of microcracks (especially when temperature exceeds 500 °C) as a result of unequal thermal expansion and thermal properties of rock-forming minerals having differing sizes [128,134,137]. These rocks are therefore unsuitable for use in high temperature TES.

Most of schists like sample SH1 can split apart into sheets at high temperature, but some others can withstand thermal cycling like samples SH2 and SH3. This is due to the non-equal schistosity. The sample SH1 has a higher degree of foliation compared to the samples SH2 and SH3.

The reasons for which the other rocks were remained mechanically stable for more than 150 thermal cycles are the following: the basalt samples BO1, BO2 et BTI, the andesite samples AAA and AHA, and the rhyolite samples RIM and RAA are volcanic rocks with fine particle sizes and cemented aspect. They are the result of rapid cooling, causing the resistance to thermal shocks. Hornfel samples HOT and AHT, and quartzite samples QZT and QID are metamorphic rocks that are formed under a combination of high temperature and high pressure. This gives them a compact structure and a good resistance to thermal cycling. Sandstone samples SO1, SO2 and SDA, dolerite sample BET, granodiorite sample GOS, gabbro samples GIM, GBH and GID, and quartzitic sandstone samples QS1-QS11 resist well to thermal cycling because they are fine-grained rocks well cemented and having small sizes of quartz mineral, leading to a resistance to the formation of microcracks in the minerals and between grains. This encourages the use of them as storage materials at high temperatures.

The results listed above are in good agreement with those of Allen et al. [128] and Homand-Etienne and Troalen [138]. The first ones used a heating rate of 2 °C/min and found that granite and quartz disintegrate during thermal cycling while the dolerite and sandstone remain stable. The second used a heating rates of 0.8–1.6 °C/min and found that limestone and granite are cracking when heated from 200 °C to 700 °C.

In the following, the thermal capacity of rocks that have withstood thermal cycling are measured and discussed.

3.2.3. Thermal capacity

The most important parameter in thermal storage applications is the heat capacity (product of specific heat capacity c_p and density ρ) which determines the ability to store sensible thermal energy [9,77]. It should be high [1,35,128] and greater than 1 MJ/m^3K [92] to reduce the storage volume required (cost) [6,31] and thermal losses from the bed, and to improve the overall efficiency of a plant.

The specific heat capacity of rock samples in powder form (particles) was measured using a differential scanning calorimeter (DSC) analysis. The equipment used is a DSC 131 Evo manufactured by Setaram. A mass of about 150 mg was used for each sample and the
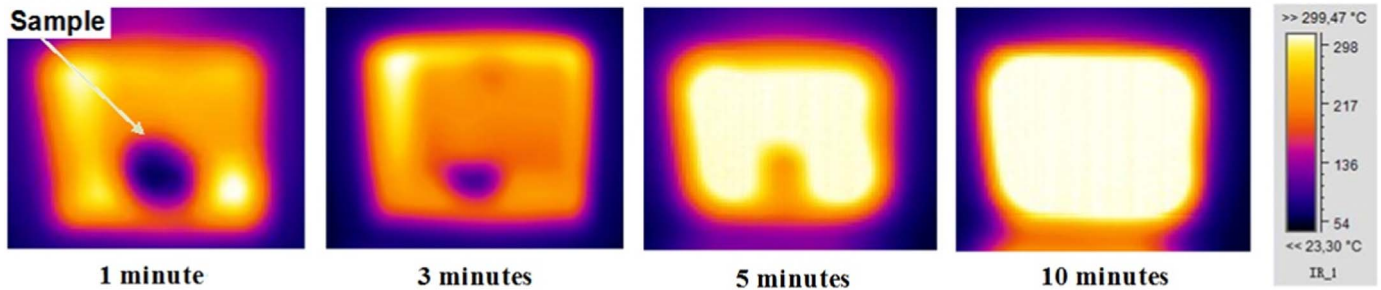
Fig. 5. Infrared photos of a rock sample in the furnace over time.

heating rate was 10 °C/min. Before being placed into the DSC, samples were accurately weighed and then placed in aluminum crucibles. The results at four different working temperatures (Table 4) show that specific heat capacity of rock increases with increasing temperature. It increases by about 60% between 25 and 500 °C. For all the samples, the heat capacity at room temperature ranges from 2.05 to 2.52 MJ/m^3 K. These values seem to be consistent with the literature as shown in Table 2.

The specific heat capacity of rock samples in solid form (bulk) was calculated using the following relationship

$$c_{p,b} = (1 - p)c_{p,p} + pc_{p,a} \qquad (2)$$

where p is the rock porosity in %. $c_{p,b}$, $c_{p,p}$ and $c_{p,a}$ are, respectively, the specific heat capacity of bulk sample, specific heat capacity of particle sample and specific heat capacity of the air. The data of specific heat capacity of the air was taken in Ref. [139] using the following relationship

$$c_{p,a} = 4,475.10^{-7}T_a^3 + 9,584.10^{-4}T_a^2 - 4,314.10^{-1}T_a + 1061 \qquad (3)$$

where T_a is the temperature of the air in Kelvin (K) and $c_{p,a}$ is in J/kg K.

In Fig. 7, thermal capacity at ambient temperature is linearly correlated with specific heat capacity of selected rocks with a coefficient of determination equal to 0.858. This is not unexpected, since the specific heat capacity values were used in calculating the thermal capacity values. The relationship between ρc_p and ρ is

$$\rho c_p = 2.2352c_p + 368.95 \qquad (4)$$

where ρ is the density in g/cm^3, c_p is the specific heat capacity in J/kg.K and ρc_p is the thermal capacity in kJ/m^3 K.

Eq. (4) is usable for predicting the thermal capacity of selected rocks from specific heat capacity data. The difference between average measured thermal capacity of selected rocks and that calculated using Eq. (4) is 46 kJ/m^3 K, which is 2% of the average measured value of 2270 kJ/m^3 K. This agrees with the results of Beck [140] which pointed out that the thermal capacity of rocks is equal to 2300 kJ/m^3 K ± 20%.

Fig. 8 shows the distribution of thermal capacities of selected rock samples. The most frequent value is situated between 2200 and 2300 kJ/m^3 K followed by that situated between 2300 and 2400 kJ/m^3 K. These values represent quite high thermal capacities that point out the suitable capacity of rocks to store the heat. Furthermore, all tested rocks have thermal capacity values greater than 2000 MJ/m^3 K, above the minimum of 1000 kJ/m^3 K suggested by Özkahraman et al. [92].

3.2.4. Thermal conductivity

Thermal conductivity describes the ability of a material to conduct heat. It is among the relevant thermo-physical properties of a storage material [10] since it improves the dynamics of charge/discharge of a storage system [6]. Xu et al. [61], Allen [79] and Meier et al. [123] reported that it is preferable to use small particles with good thermal conductivity so that the inner volume of the rock may heat up or cool down completely during the charging and discharging process and for better thermal stratification (see Fig. 9). Thermal stratification increases the efficiency of thermal cycling [141] and thermal storage [142]. It can be achieved for high conductivity inside the particles and lower conductivity between adjacent particles in axial direction. Singh et al. [143] found that the stratification coefficient is maximum for a bed of spheres. Xu et al. [61] reported that to obtain high discharging efficiency, the thermal conductivity of solid particles must be high, but it should not be large to avoid raising thermal conduction between particles. Furthermore, with high thermal conductivity, the rate of charging and discharging will be much faster [79,144] thereby increasing the thermal performance of TES [25]. In other words, to ensure efficient heat transfer between HTF and rock [145], it is necessary to make reference to the Biot number (Bi). If the Bi is less than 0.1, it means that the internal resistance is negligible and the temperature distribution in the rock is uniform [120,142]. Saez and McCoy [146] found that, if Bi «1, the temperature of the fluid and that of the solid in packed bed will be identical. So, it is better to use small particles with nearly spherical shape and good thermal conductivity (> 1 W/m K) which means having a Bi less than about 0.1.

Average thermal conductivity values taken from literature are presented in Table 2. Using the equation developed by Zoth and Hanel [147], we can presented thermal conductivity as a function of temperature for different rock types (Fig. 10). From Table 2 and Fig. 10, it can be concluded that rocks have good values of thermal conductivity.

In general, for most rocks and minerals, thermal conductivity decreases with increase in temperature [42,44,148] and increases with increase in quartz content [149] and density [150]. Seipold [151]
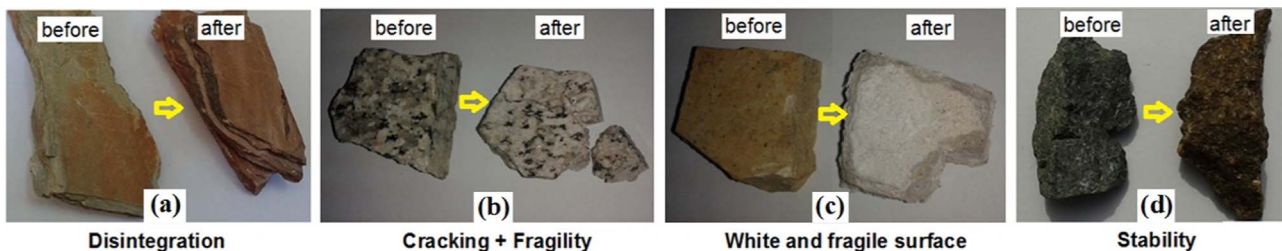

Fig. 6. The important statuses of rocks after thermal cycling: (a) Degradation of schist sample SH1 by separation of layers, (b) cracking of granite sample GT2, (c) formation of white layer to the surface of marble sample MBT and stability of gabbro sample GID.

Table 4
Calculated energy storage density and measured specific heat capacity of selected rocks at four different temperatures.

| Sample	c_p (J/kg K) (25 °C)		ρc_p (kJ/m³K) (25 °C)	ρc_p (kWh/m³K) (25 °C)	Energy storage density (kWh/m³) ($\Delta T = 400$ °C)	c_p (J/kg K) (100 °C)		c_p (J/kg K) (300 °C)		c_p (J/kg K) (500 °C)	
	Particle	Bulk				Particle	Bulk	Particle	Bulk	Particle	Bulk
BET	864.8	869.8	2361	0.6559	262.3	921.2	925.3	1040.5	1045.8	1114.2	1126.2
GOS	822.5	831.3	2266	0.6297	251.8	896.3	903.1	1047.5	1054.5	1131.4	1147.4
BO1	837.3	848.4	2274	0.6318	252.7	890.8	900.4	1015.2	1026.6	1111.5	1134.3
BO2	816.8	819.5	2180	0.6057	242.2	874.4	876.7	1001.8	1004.5	1091.2	1096.5
BTI	825.9	842.3	2208	0.6134	245.3	884.4	898.3	999.2	1016.4	1052.3	1088.9
RIM	829.8	830.7	2193	0.6091	243.6	877.3	878.1	999.1	1000.0	1113.3	1115.0
RAA	811.1	819.0	2130	0.5917	236.6	874.8	881.4	1017.3	1024.3	1118.6	1132.6
AAA	847.0	856.9	2327	0.6464	258.5	902.0	910.4	1014.2	1025.0	1075.1	1098.5
AHA	818.7	833.2	2212	0.6144	245.7	874.4	886.9	978.1	994.2	1015.8	1049.5
GIM	776.3	779.1	2231	0.6198	247.9	838.7	841.1	955.4	958.3	999.9	1005.5
GBH	836.3	841.6	2242	0.6227	249.1	898.0	902.3	1037.0	1041.8	1138.7	1148.7
GID	750.0	756.4	2052	0.5700	228.0	858.3	862.8	1045.9	1049.7	1086.0	1095.6
SO1	920.5	923.5	2440	0.6780	271.2	959.8	962.4	1034.5	1039.3	1065.1	1077.0
SO2	856.2	866.0	2219	0.6165	246.6	898.6	907.5	1008.6	1020.1	1113.2	1135.4
SDA	923.6	932.7	2318	0.6440	257.6	941.9	951.8	1034.9	1050.2	1190.2	1217.4
HOT	832.0	846.9	2258	0.6274	250.9	909.9	920.9	1062.1	1073.4	1132.1	1160.3
AHT	949.9	954.8	2476	0.6879	275.1	984.2	988.7	1044.9	1055.3	1059.6	1087.2
SH2	891.2	898.4	2388	0.6635	265.4	921.9	928.9	1024.1	1033.9	1155.2	1173.4
SH3	869.9	890.3	2306	0.6407	256.3	916.2	934.1	1035.5	1058.1	1146.5	1192.5
QZT	768.9	773.6	2050	0.5694	227.7	848.0	851.8	1023.3	1026.7	1146.0	1152.5
QID	806.7	809.0	2103	0.5842	233.7	886.3	888.1	1054.9	1056.6	1160.1	1163.7
QS1	915.0	915.5	2527	0.7021	280.8	968.5	968.9	1083.9	1084.5	1159.5	1161.0
QS2	877.7	878.5	2412	0.6701	268.0	929.1	929.8	1020.5	1021.5	1045.5	1047.9
QS3	858.4	859.1	2384	0.6624	264.9	918.1	918.7	1045.4	1046.1	1126.2	1127.7
QS4	871.0	874.2	2334	0.6483	259.3	915.3	918.2	1025.9	1029.7	1125.0	1132.7
QS5	883.4	887.2	2386	0.6629	265.1	923.6	927.1	1029.4	1034.2	1132.8	1142.6
QS6	823.7	826.3	2232	0.6201	248.0	882.0	884.2	991.1	993.9	1032.7	1038.6
QS7	835.0	836.4	2341	0.6505	260.2	892.9	894.1	1008.2	1009.7	1066.4	1069.6
QS8	819.8	820.9	2214	0.6152	246.0	884.8	885.7	997.4	998.5	1021.6	1024.0
QS9	835.8	839.3	2224	0.6180	247.2	890.6	893.6	999.2	1003.1	1052.8	1061.1
QS10	849.0	855.0	2265	0.6293	251.7	916.4	921.0	1045.6	1051.1	1100.7	1114.0
QS11	803.1	808.1	2105	0.5847	233.9	868.7	872.9	995.4	1000.2	1051.3	1061.4
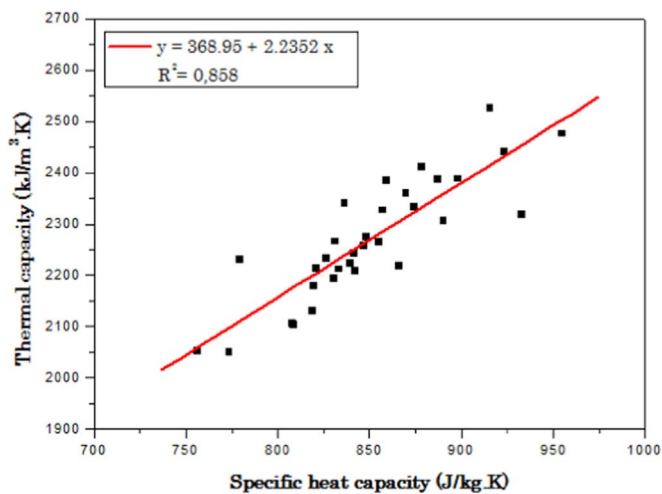
Fig. 7. Thermal capacity versus specific heat capacity of selected rocks.
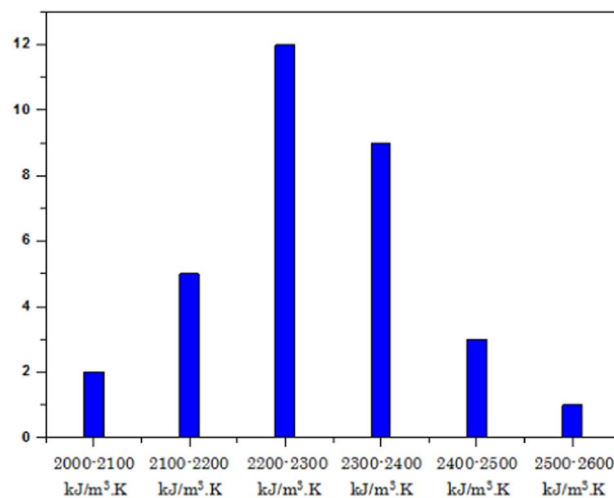

Fig. 8. Frequency distribution of thermal capacities.

indicated that when a rock has high thermal conductivity at room temperature, the decrease with temperature will be stronger.

The obtained results of thermal and physico-mechanical properties, and the literature review show that all the studied rocks are suitable for low temperature thermal storage, but the results of thermal cycling show that some rock samples are suitable for high temperature and the others did not, which necessitated to be removed from the list of studied rocks in order to avoid any damages in the storage unit. In Figs. 11 and 12, the thermal conductivity and hardness are plotted as a function of thermal capacity. Thermal conductivity data are based on the literature

values given in Table 2. As can be seen, gabbro, quartzitic sandstone, dolerite, granodiorite and hornfels are those that combine the best properties. Most of thermal capacity values at 300 °C are located between 2700 and 2900 kJ/m³ K, which proves the suitability of rocks in thermal storage. The highest thermal capacity at room temperature is related to the quartzitic sandstone QS1 (2527 kJ/m³ K). In term of energy storage density (Table 4), dolerite sample BET, sandstone sample SO1, schist sample SH2, hornfels sample AHT and quartzitic sandstone samples QS1, QS2, QS3 and QS5 are the optimal rocks.

It is evident from this article and previous articles that quartz is the
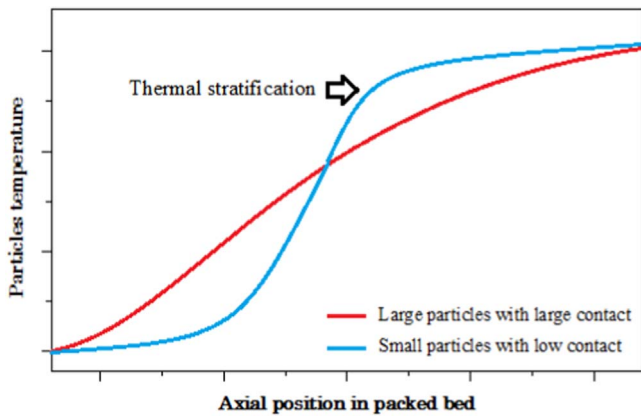
Fig. 9. Effect of particles diameter and contact between particles on the thermal stratification.
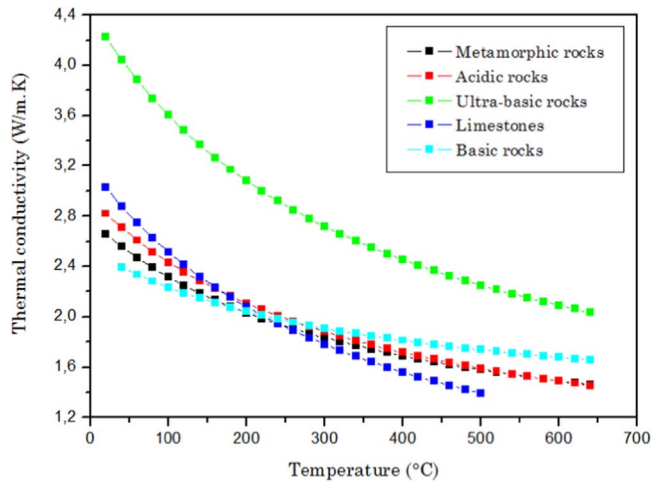

Fig. 12. Hardness versus thermal capacity at 300 °C.

Fig. 10. Thermal conductivity of different rock types as a function of temperature [147].

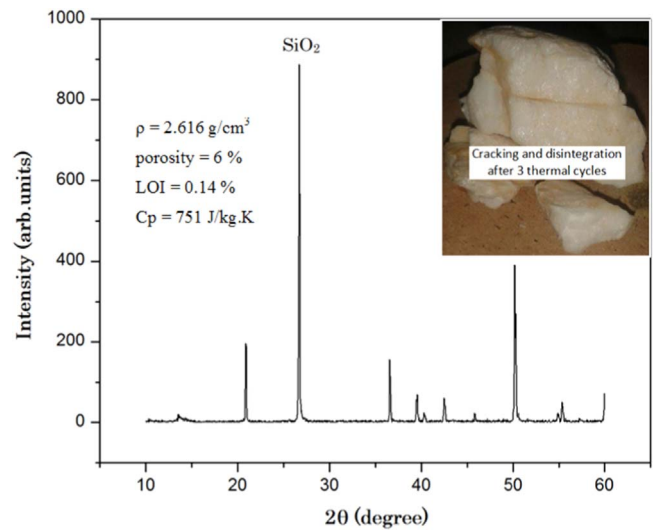**Fig. 13.** X-ray diffraction spectrum of quartz and other thermophysical properties.

negatively affect thermal cycling resistance of rocks containing quartz with larger sizes. Fig. 13 shows the X-ray diffraction spectrum of an amorphous quartz from Tafraoute region (Anti-Atlas). The results of thermal cycling and some other measured thermo-physical properties were inserted in the Figure. The other peaks observed in the spectrum are due to the traces of quartz.

4. Conclusion

Thermal energy storage is a promising technology that enhances the efficiency of renewable energies. This paper demonstrates the potential of rocks as candidate materials for high temperature thermal storage. Based on the literature review and from the economic point of view, natural rock can be used as very promising storage material for large-scale CSP systems and especially when air is used as heat transfer fluid.

A variety of rock samples have been tested in this paper and the studied parameters vary considerably within the same rock type. The thermal cycling tests show that not all rocks are suitable for high temperature storage. Some rock types have been damaged at high temperatures. Based on these results and according to various criteria, dolerite, granodiorite, hornfels, gabbro and quartzitic sandstone are the best candidate to be implemented in a high temperature storage system.

Fig. 11. Thermal conductivity versus thermal capacity.

main mineral influencing rock properties. It is known by its high thermal conductivity (7.7 W/mK) [152] compared to others rock-forming minerals. Rocks with higher content of quartz can have conductivities of about 3–5 W/m K [153]. Quartz has a large and anisotropic thermal expansion as well as a large hardness. Furthermore, materials including quartz are susceptible to rapid increase in volume due to the α-β quartz transition [136,154]. This transition (expansion)

Acknowledgements

References

[1] A.I. Fernandez, M. Martinez, M. Segarra, I. Martorell, L.F. Cabeza, Selection of materials with potential in sensible thermal energy storage, Sol. Energy Mater. Sol. Cells 94 (2010) 1723–1729.

[2] S. Khare, M. Dell'Amico, C. Knight, S. McGarry, Selection of materials for high temperature sensible energy storage, Sol. Energy Mater. Sol. Cells 115 (2013) 114–122.

[3] L.F. Cabeza, E. Galindo, C. Prieto, C. Barreneche, A.I. Fernandez, Key performance indicators in thermal energy storage: survey and assessment, Renew. Energy 83 (2015) 820–827.

[4] L. Geissbuhler, M. Kolman, G. Zanganeh, A. Haselbacher, A. Steinfeld, Analysis of industrial-scale high-temperature combined sensible/latent thermal energy storage, Appl. Therm. Eng. 101 (2016) 657–668.

[5] E. Oró, A. Gil, A. de Gracia, D. Boer, L.F. Cabeza, Comparative life cycle assessment of thermal energy storage systems for solar power plants, Renew. Energy 44 (2012) 166–173.

[6] M.E. Navarro, M. Martinez, A. Gil, A.I. Fernandez, L.F. Cabeza, R. Olives, X. Py, Selection and characterization of recycled materials for sensible thermal energy storage, Sol. Energy Mater. Sol. Cells 107 (2012) 131–135.

[7] D. Okello, C.W. Foong, O.J. Nydal, E.J.K. Banda, An experimental investigation on the combined use of phase change material and rock particles for high temperature (350 °C) heat storage, Energy Convers. Manag. 79 (2014) 1–8.

[8] S.M. Hasnain, Review on sustainable thermal energy storage technologies, Part I: heat storage materials and techniques, Energy Convers. Manag. 39 (1998) 1127–1138.

[9] K. Ismail, R. Stuginsky, A parametric study on possible fixed bed models for pcm and sensible heat storage, Appl. Therm. Eng. 19 (7) (1999) 757–788.

[10] B. Zalba, J.M. Marin, L.F. Cabeza, H. Mehling, Review on thermal energy storage with phase change: materials, heat transfer analysis and applications, Appl. Therm. Eng. 23 (2003) 251–283.

[11] M.M. Kenisarin, High-temperature phase change materials for thermal energy storage, Renew. Sustain. Energy Rev. 14 (2010) 955–970.

[12] A. Gil, M. Medrano, I. Martorell, A. Lazaro, P. Dolado, B. Zalba, L.F. Cabeza, State of the art on high temperature thermal energy storage for power generation. Part 1—concepts, materials and modellization, Renew. Sustain. Energy Rev. 14 (2010) 31–55.

[13] E. Oró, A. de Gracia, A. Castell, M.M. Farid, L.F. Cabeza, Review on phase change materials (PCMs) for cold thermal energy storage applications, Appl. Energy 99 (2012) 513–533.

[14] J. Cot-Gores, A. Castell, L.F. Cabeza, Thermochemical energy storage and conversion: a-state-of-the-art review of the experimental research under practical conditions, Renew. Sustain. Energy Rev. 16 (2012) 5207–5224.

[15] S. Kuravi, J. Trahan, D.Y. Goswami, M.M. Rahman, E.K. Stefanakos, Thermal energy storage technologies and systems for concentrating solar power plants, Prog. Energy Combust. Sci. 39 (2013) 285–319.

[16] G. Zanganeh, M. Commerford, A. Haselbacher, A. Pedretti, A. Steinfeld, Stabilization of the outflow temperature of a packed-bed thermal energy storage by combining rocks with phase change materials, Appl. Therm. Eng. 70 (2014) 316–320.

[17] X. Liu, C. Lin, Z. Rao, Diffusion and thermal conductivity of the mixture of paraffin and polystyrene for thermal energy storage: a molecular dynamics study, J. Energy Inst. (2016) 1–10.

[18] A. Dinker, M. Agarwal, G.D. Agarwal, Heat storage materials, geometry and applications: a review, J. Energy Inst. (2015) 1–11.

[19] L. Navarro, A. de Gracia, S. Colclough, M. Browne, S.J. McCormack, P. Griffiths, L.F. Cabeza, Thermal energy storage in building integrated thermal systems: a review. Part 1. active storage systems, Renew. Energy 88 (2016) 526–547.

[20] M.J. Huang, P.C. Eames, S. McCormack, P. Griffiths, N.J. Hewitt, Microencapsulated phase change slurries for thermal energy storage in a residential solar energy system, Renew. Energy 36 (2011) 2932–2939.

[21] S. Almsater, W. Saman, F. Bruno, Performance enhancement of high temperature latent heat thermal storage systems using heat pipes with and without fins for concentrating solar thermal power plants, Renew. Energy 89 (2016) 36–50.

[22] G. Peiro, J. Gasia, L. Miro, L.F. Cabeza, Experimental evaluation at pilot plant scale of multiple PCMs (cascaded) vs. single PCM configuration for thermal energy storage, Renew. Energy 83 (2015) 729–736.

[23] J. Zhao, Y. Guo, F. Feng, Q. Tong, W. Qv, H. Wang, Microstructure and thermal properties of a paraffin/expanded graphite phase-change composite for thermal storage, Renew. Energy 36 (2011) 1339–1342.

[24] P. Sobolciak, M. Karkri, M.A. Al-Maadeed, I. Krupa, Thermal characterization of phase change materials based on linear low-density polyethylene, paraffin wax and expanded graphite, Renew. Energy 88 (2016) 372–382.

[25] J. Gasia, L. Miró, L.F. Cabeza, Materials and system requirements of high temperature thermal energy storage systems: a review. Part 2: thermal conduc-

[25] tivity enhancement techniques, Renew. Sustain. Energy Rev. 60 (2016) 1584–1601.

[26] F. Agyenim, N. Hewitt, P. Eames, M. Smyth, A review of materials, heat transfer and phase change problem formulation for latent heat thermal energy storage systems (LHTESS), Renew. Sustain. Energy Rev. 14 (2) (2010) 615–628.

[27] S. Pincemin, Elaborations et caractérisations de matériaux composites à hautes performances énergétiques pour l'intégration d'un stockage thermique dans les centrales électrosolaires (PhD), Université de Perpignan, 2007.

[28] J.C. Hadorn, Thermal energy storage for solar and low energy buildings, state of art by the IEA Solar Heating and Cooling Programme Task 32, 2005.

[29] H. Singh, R.P. Saini, J.S. Saini, A review on packed bed solar energy storage systems, Renew. Sustain. Energy Rev. 14 (2010) 1059–1069.

[30] A. Kumar, S.K. Shukla, A review on thermal energy storage unit for solar thermal power plant application, Energy Procedia 74 (2015) 462–469.

[31] R. Anderson, S. Shiri, H. Bindra, J.F. Morris, Experimental results and modeling of energy storage and recovery in a packed bed of alumina particles, Appl. Energy 119 (2014) 521–529.

[32] J. Xu, R.Z. Wang, Y. Li, A review of available technologies for seasonal thermal energy storage, Sol. Energy 103 (2014) 610–638.

[33] J.A. Duffie, W.A. Beckman, Solar Engineering for Thermal Processes, John Wiley and Sons, Inc, 2006.

[34] O.E. Ataer, Storage of thermal energy, in: Y.A. Gogus (Ed.), Energy Storage Systems, EOLSS, Publishers, Oxford, UK, 2006.

[35] L.F. Cabeza, I. Martorell, L. Miró, A.I. Fernández, C. Barreneche, Introduction to thermal energy storage (TES) systems, Adv. Therm. Energy Storage Syst.: Methods Appl. 1 (2014).

[36] F. Dinter, Thermische Energiespeicher in Solarkraftwerken und ihre Bewertung. Aachen: Verlag Shaker, 1992.

[37] D.J. Matyas, T. Ohji, X. Liu, M.P. Paranthaman, R. Devanathan, K. Fox, M. Singh, W. Wong-ng, Advances in Materials Science for Environmental and Energy Technologies II, Ceramic Transactions 241 John Wiley & Sons, 2013.

[38] F.P. Incropera, D.P. Dewitt, Fundamentals of Heat and Mass Transfer, Wiley, New York, 1990.

[39] D.W. Waples, J.S. Waples, A review and evaluation of specific heat capacities of rocks, minerals, and subsurface fluids. Part1: minerals and nonporous rocks, Nat. Resour. Res. 13 (2) (2004) 97–122.

[40] B.V. Gokhale, Rotary Drilling and Blasting in Large Surface Mines, CRC Press/Balkema, London, UK, 2011.

[41] V. Pasquale, M. Verdoya, P. Chiozzi, Measurements of rock thermal conductivity with a Transient Divided Bar, Geothermics 53 (2015) 183–189.

[42] S.Q. Miao, H.P. Li, G. Chen, Temperature dependence of thermal diffusivity, specific heat capacity, and thermal conductivity for several types of rocks, J. Therm. Anal. Calorim. 115 (2014) 1057–1063.

[43] H. Grirate, N. Zari, Iz Elamrani, R. Couturier, A. Elmchaouri, S. Belcadi, P. Tochon, Characterization of several Moroccan rocks used as filler material for thermal energy storage in CSP power plants, Energy Procedia 49 (2014) 810–819.

[44] L. Eppelbaum, I. Kutasov, A. Pilchin, Thermal properties of rocks and density of fluids, In Applied Geothermics, Springer Berlin Heidelberg, 2014 (99-14).

[45] T. Andolfsson, (hp), Analyses of thermal conductivity from mineral composition and analyses by use of Thermal Conductivity Scanner: A study of thermal properties in Scanian rock types No. 361 Dissertations in Geology at Lund University, 2013, p. 45.

[46] The engineering toolbox, Solids: specific heat capacities and thermal conductivities, Available in: ⟨http://www.engineeringtoolbox.com/⟩, 2016.

[47] W.J. Cho, S. Kwon, Estimation of the thermal properties for partially saturated granite, Eng. Geol. 115 (2010) 132–138.

[48] POIC, PO Ingénierie de la Construction, Chapitre 2, Pétrographie, Géologie de l'ingénieur, Toulouse: INSA, Available in: ⟨https://moodle.insa-toulouse.fr⟩, 2015.

[49] F.J. Janza, Interaction mechanisms, Man. Remote Sens. 1 (1975) 75–179.

[50] F. Birch, H. Clark, The thermal conductivity of rocks and its dependence upon temperature and composition, Am. J. Sci. 238 (8) (1940) 529–558.

[51] P.V. Sharma, Environmental and Engineering Geophysics, Cambridge UniversityPress, Cambridge, 2002.

[52] C.S. Blázquez, A.F. Martín, I.M. Nieto, P.C. García, L.S.S. Pérez, D.G. Aguilera, Thermal conductivity map of the Avila region (Spain) based on thermal conductivity measurements of different rock and soil samples, Geothermics 65 (2017) 60–71.

[53] Y.M. Proselkov, Heat transfer in wells. Nedra, Moscow (in Russian), 1975.

[54] P.K. Dehdezi, Enhancing Pavements for Thermal Applications. Department of Civil Engineering Nottingham Transportation Engineering Centre, Thesis submitted to the University of Nottingham, 2012.

[55] G. Zanganeh, A. Pedretti, S. Zavattoni, M. Barbato, A. Steinfeld, Packed-bed thermal storage for concentrated solar power – Pilot-scale demonstration and industrial-scale design, Sol. Energy 86 (2012) 3084–3098.

[56] I.I. Stylianou, S. Tassou, P. Christodoulides, I. Panayides, G. Florides, Measurement and analysis of thermal properties of rocks for the compilation of geothermal maps of Cyprus, Renew. Energy 88 (2016) 418–429.

[57] J. Zhao, Rock Mechanics Mécanique des roches. Course Lectures, 2ème partie – mécanique et propriétés des massifs rocheux, 2007.

[58] S.P. Clark (Ed.), Handbook of Physical Constants, 97 Geological Society of America, 1966.

[59] E.C. Robertson, Thermal conductivity of rocks, U.S. Geological Survey open file report (1979), pp. 79–356.

[60] N. Mertens, F. Alobaid, L. Frigge, B. Epple, Dynamic simulation of integrated rock-bed thermocline storage for concentrated solar power, Sol. Energy 110 (2014)

[60] 830–842.

[61] C. Xu, X. Li, Z. Wang, Y. He, F. Bai, Effects of solid particle properties on the thermal performance of a packed-bed molten-salt thermocline thermal storage system, Appl. Therm. Eng. 57 (2013) 69–80.

[62] J.F. Hoffmann, Stockage thermique pour centrale solaire thermodynamique à concentration mettant en oeuvre des matériaux céramiques naturels ou recyclés, Doctoral dissertation, Perpignan, 2015.

[63] D. Barry-Macaulay, A. Bouazza, R.M. Singh, B. Wang, P.G. Ranjith, Thermal conductivity of soils and rocks from the Melbourne (Australia) region, Eng. Geol. 164 (2013) 131–138.

[64] D. Koňáková, E. Vejmelková, R. Černý, Thermal properties of selected sandstones, in: Proceedings of the 4th International Conference on Fluid Mechanics and Heat & Mass Transfer, 2013.

[65] A.O. Guimarães, D.A. Viana, T.C. Cordeiro, J.A. Sampaio, E.C. da Silva, R. Toledo, H.J.P.S. Ribeiro, A.A.G. Carrasquilla, H. Vargas, On the use of photothermal methods for thermal characterization of sedimentary rocks from the Paraná Basin in Brazil, Mari. Petrol. Geol. 43 (2013) 121–126.

[66] M.G. Alishaev, I.M. Abdulagatov, Z.Z. Abdulagatova, Effective thermal conductivity of fluid-saturated rocks experiment and modeling, Eng. Geol. 135 (2012) 24–39.

[67] P.E. Back, J. Wrafter, J. Sundberg, Thermal properties, Site descriptive modeling Forsmark-stage 2.2, Swedish Nuclear Fuel and Waste Management Co, Box 5864, SE-102 40 Stockholm Sweden, 2007.

[68] R.D. Hyndman, M.J. Drury, Physical properties of basalts, gabbros and ultramafic rocks from DSDP LEG 37, DSDP 37 (1977) 395–401.

[69] A. Aurangzeb, Prediction of effective thermal conductivity of gabbro rocks under ambient conditions, 2009.

[70] D. Mottaghy, H.D. Vosteen, R. Schellschmidt, Temperature dependence of the relationship of thermal diffusivity versus thermal conductivity for crystalline rocks, Int. J. Earth Sci. 97 (2) (2008) 435–442.

[71] K. Horai, Thermal conductivity of sediments and igneous rocks recovered during Deep-Sea Drilling Project LEG-60, Initial Rep. Deep Sea Drill. Proj. 60 (1982) 807–834.

[72] British Geological Survey, s.a., GeoReports, October, Available in: ⟨https://shop.bgs.ac.uk/GeoReports/examples/modules/C011.pdf⟩, 2014.

[73] R. Tiskatine, A. Eddemani, L. Gourdo, B. Abnay, A. Ihlal, A. Aharoune, L. Bouirden, Experimental evaluation of thermo-mechanical performances of candidate rocks for use in high temperature thermal storage, Appl. Energy 171 (2016) 243–255.

[74] August Wikipedia, Available in: ⟨https://www.wikipedia.org/⟩, 2016.

[75] N. Bagdassarov, D. Dingwell, Thermal properties of vesicular rhyolite, J. Volcan. Geotherm. Res. 60 (2) (1994) 179–191.

[76] A.F. Elhakim, The use of point load test for Dubai weak calcareous sandstones, J. Rock. Mech. Geotech. Eng. 7 (4) (2015) 452–457.

[77] M. Hänchen, S. Brückner, A. Steinfeld, High temperature thermal storage using a packed bed of rocks-Heat transfer analysis and experimental validation, Appl. Therm. Eng. 31 (2011) 1798–1806.

[78] Tulikivi, Poropriétés de la Stéatite, August, Available in: ⟨http://www.tulikivi.com/fr/Tulikivi/La_steatite_Proprietes_de_la_steatite⟩, 2016.

[79] K. Allen, Performance Characteristics of Packed Bed Thermal Energy Storage for Solar thermal power plants, (Master's thesis) University of Stellenbosch, 2010.

[80] D. Laing, S. Zunft, Using concrete and other solid storage media in thermal energy storage (TES) systems, Adv. Therm. Energy Storage Syst. (2015) 65–86.

[81] Y. Jemmal, N. Zari, M. Maaroufi, Thermophysical and chemical analysis of gneiss rock as low cost candidate material for thermal energy storage in concentrated solar power plants, Sol. Energy Mater. Sol. Cells 157 (2016) 377–382.

[82] P. Eloranta, Onkalo Pose Experiment - Uniaxial compressive strength test results: 120 mm diameter samples from the experimental holes, Posiva OY, Working Report, 2015.

[83] A.S.A. Ammar, A.A. Ghoneim, Optimization of a sensible heat storage unit packed with spheres of a local material, Renew. Energy 1 (1) (1991) 91–95.

[84] G.A. Anikoh, B.M. Olaleye, Estimation of strength properties of shale from Some of its physical properties using developed mathematical models, Int. J. Eng. Sci. 2 (4) (2013) 1–5.

[85] D.D. Blackwell, J.L. Steele, Thermal conductivity of sedimentary rocks: measurement and significance, in: N.D. Naeser, T.H. McCulloch (Eds.), Thermal History of Sedimentary Basins, Springer, New York, 1989, pp. 5–96.

[86] Densities of Common Rocks and Minerals, November, Available in: ⟨http://geology.about.com/⟩, 2016.

[87] O. Kappelmeyer, R. Haenel, Geothermics with special reference to applications: Gebruder Borntraeger, Berlin, 238 p, 1974.

[88] V.A. Salomoni, C.E. Majorana, G.M. Giannuzzi, A. Miliozzi, R. Di Maggio, F. Girardi, D. Mele, M. Lucentini, Thermal storage of sensible heat using concrete modules in solar power plants, Sol. Energy 103 (0) (2014) 303–315.

[89] ISO, E. 10456, Building materials and products, Hygrothermal properties, Tabulated design values and procedures for determining declared and design thermal values, Brussels: CEN, 2007.

[90] D. Laing, W.D. Steinmann, R. Tamme, C. Richter, Solid media thermal storage for parabolic trough power plants, Sol. Energy 80 (2006) 1283–1289.

[91] Z.P. Bazant, J.C. Chern, M.S. Abrams, M.P. Gillen, Normal and Refractory Concretes for LMFBR Applications -Vol. 2, Evaluation of concretes for LMFBR Applications, Electric Power Research Institute Technical Report NP-2437, 2, 1982.

[92] H.T. Özkahraman, R. Selver, E.C. Isik, Determination of the thermal conductivity of rock from P-wave velocity, Int. J. Rock. Mech. Min. Sci. 41 (4) (2004) 703–708.

[93] Y. Xu, D.D.L. Chung, Effect of sand addition on the specific heat and thermal conductivity of cement, Cem. Concr. Res. 30 (2000) 59–61.

[94] Z. Ma, M. Mehos, G. Glatzmaier, B.B. Sakadjian, Development of a concentrating solar power system using fluidizedbed technology for thermal energy conversion and solid particles for thermal energy storage, Energy Procedia 69 (2015) 1349–1359.

[95] I. Ortega, A. Faik, A. Gil, J. Rodríguez-Aseguinolaza, B. D'Aguanno, Thermo physical properties of a steel-making by-product to be used as thermal energy storage material in a packed-bed system, Energy Procedia 69 (2015) 968–977.

[96] E. Wasserman, L. Stixrude, R.E. Cohen, Thermal properties of iron at high pressures and temperatures, Phys. Rev. B 27 (1996) 312–356.

[97] X. Py, N. Calvet, R. Olivès, P. Echegut, C. Bessada, F. Jay, Thermal storage for solar power plants based on low cost recycled material. EFFSTOCK, in: Proceedings of the 11th International Conference on Thermal Energy Storage, June, 2009.

[98] R. Gutiérrez, H. García, B. Cardenas, N. León, Material selection for Latent heat based high temperature solar thermal energy storage, Energy Procedia 74 (2015) 1525–1532.

[99] Y. Nagasaka, A. Nagashima, The thermal conductivity of molten $NaNO_3$ and KNO_3, Int. J. Thermophys. 12 (5) (1991) 769–781.

[100] Thermal energy storage, Technology Brief, Available in: ⟨http://www.irena.org/Publications⟩, 2015.

[101] H. Ibrahim, A. Ilinca, J. Perron, Energy storage systems-characteristics and comparison, Renew. Sustain. Energy Rev. 12 (2008) 1221–1250.

[102] Civil Engineering, August, Available in: ⟨http://civiltoday.com/civil-engineering-materials/concrete/15-advantages-and-disadvantages-of-concrete⟩, 2016.

[103] In solid Share, Castable ceramics/ dentistry training, August 2016, Available in: ⟨http://fr.slideshare.net/indiandentalacademy/castable-ceramics-rohit⟩.

[104] Pumps, Systems August, Available in: ⟨http://www.pumpsandsystems.com/topics/bearings/trouble-silicon-carbide⟩, 2016.

[105] Ceram, and Refractories, Available in: ⟨http://www.ceram-refractories.com/⟩, 2015.

[106] VITCAS, August, Available in: ⟨http://www.vitcas.com/refractory-fire-bricks⟩, 2016.

[107] N. Mahfoudi, Stockage de la chaleur dans un milieu granuleux solide, Doctoral dissertation, Université Mohamed Khider de Biskra, 2016.

[108] Les laitiers sidérurgiques, CTPL, November, Available in: ⟨http://www.ctpl.info/presentation/les-laitiers-siderurgiques/⟩, 2016.

[109] A. Sowbhagy, M. Rao, K. Narender, Thermophysical properties of NaCl, NaBr and NaF by γ-ray attenuation technique, J. Mod. Phys. 4 (2013) 208–214.

[110] H. Michels, R. Pitz-Paal, Cascaded latent heat storage for parabolic trough solar power plants, Sol. Energy 81 (2007) 829–837.

[111] E.G. Kovach, Thermal Energy Storage: The Report of a NATO Science Committee Conference Held at Turnberry, Scotland, 1st-5th March 1976, Pergamon Press, 2013.

[112] D. Brosseau, J.W. Kelton, D. Ray, M. Edgar, K. Chisman, B. Emms, Testing of thermocline filler materials and molten-salt heat transfer fluids for thermal energy storage systems in parabolic trough power plants, J. Sol. Energy Eng. 127 (1) (2005) 109–116.

[113] D.R. Mills, J. Gordon (Ed.), Solar Thermal Electricity, The State of the Art ISES Position Papers, Cromwell Press, United Kingdom, 2001.

[114] G. Zanganeh, A. Pedretti, A. Haselbacher, A. Steinfeld, Design of packed bed thermal energy storage systems for high-temperature industrial process heat, Appl. Energy 137 (2015) 812–822.

[115] P.L. Singh, S.D. Deshpandey, P.C. Jena, Thermal performance of packed bed heat storage system for solar air heaters, Energy Sustain. Dev. 29 (2015) 112–117.

[116] C.J. Coetzee, R.G. Nel, Calibration of discrete element properties and the modelling of packed rock beds, Powder Technol. 264 (2014) 332–342.

[117] N.G. Barton, Simulations of air-blown thermal storage in a rock bed, Appl. Therm. Eng. 55 (2013) 43–50.

[118] H.W. Fricker, High temperature heat storage using natural rock, Sol. Energy Mater. 24 (1991) 249–254.

[119] G. Zanganeh, High-Temperature Thermal Energy Storage for Concentrated Solar Power with Air as Heat Transfer Fluid, Doctoral dissertation, Diss., Eidgenössische Technische Hochschule ETH Zürich, Nr. 21802, 2014.

[120] J.P. Coutier, E.A. Farber, Two application of a numerical approach of heat transfer process within rock beds, Sol. Energy 29 (1982) 451–462.

[121] J. Liu, L. Wang, L. Yang, L. Yue, L. Chai, Y. Sheng, H. Chen, C. Tan, Experimental study on heat storage and transfer characteristics of supercritical air in a rock bed, Int. J. Heat. Mass Trans. 77 (2014) 883–890.

[122] L. Heller, P. Gauché, Modeling of the rock bed thermal energy storage system of a combined cycle solar thermal power plant in South Africa, Sol. Energy 93 (2013) 345–356.

[123] A. Meier, C. Winkler, D. Wuillemin, Experiment for modelling high temperature rock bed storage, Sol. Energy Mat. 24 (1991) 255–264.

[124] P.A. Curto, G. Stern, Thermal storage using slag, Alt. Energy 3 (1) (1980) 195–208.

[125] D.E. Beasley, J.A. Clark, Transient response of a packed bed for thermal energy storage, Int. J. Heat Mass Transf. 27 (9) (1984) 1659–1669.

[126] K. Sagara, N. Nakahara, Thermal performance and pressure drop of rock beds with large storage materials, Sol. Energy 47 (3) (1991) 157–163.

[127] J.E. Pacheco, S.K. Showalter, W.J. Kolb, Development of a Molten-Salt Thermocline Thermal Storage System for Parabolic Trough Plants, J. Sol. Energy Eng. 124 (2002) 153–159.

[128] K.G. Allen, T.W. v. onBackstrom, D.G. Kroger, A.F.M. Kisters, rock bed storage for solar thermal power plants: rock characteristics, suitability, and availability, Sol. Energy Mater. Sol. Cells 126 (2014) 170–183.

[129] S.A. Zavattoni, M.C. Barbato, A. Pedretti, G. Zanganeh, Evaluation of thermal stratification of an air-based thermocline TES with low-cost filler material, Energy

Procedia 73 (2015) 289–296.

[130] H. Grirate, H. Agalit, N. Zari, A. Elmchaouri, S. Molina, R. Couturier, Experimental and numerical investigation of potential filler materials for thermal oil thermocline storage, Sol. Energy 131 (2016) 260–274.

[131] W.F. Brace, Dependence of fracture strength of rocks on grain size, in: Proceedings of the Fourth Symposium on Rock Mechanics, University of Park, Pennsylvania, PA 99–103, 1961.

[132] N.J. Price, The compressive strength of coal measure rocks, CollEng 37 (1960) 283–292.

[133] M.I. Smorodinov, E.A. Motovilov, V.A. Volkov, Determinations of correlation relationships between strength and some physical characteristics of rocks, Proceedings of the Second Congress of the International Society of Rock Mechanics, vol. 2. Belgrade 35-37, 1970.

[134] W. Zhang, Q. Sun, S. Hao, J. Geng, C. Lv, Experimental study on the variation of physical and mechanical properties of rock after high temperature treatment, Appl. Therm. Eng. 98 (2016) 1297–1304.

[135] B. Menendez, C. David, M. Darot, A study of the crack network in thermally and mechanically cracked granite samples using confocal scanning laser microscopy, Phys. Chem. Earth 24 (7) (1999) 627–632.

[136] T. Huotari, I. Kukkonen, Thermal expansion properties of rocks: Literature survey and estimation of thermal expansion coefficient for Olkiluoto mica gneiss, Posiva Oy, Olkiluoto, Working Report, 4 62, 2004.

[137] E.C. David, N. Brantut, A. Schubnel, R.W. Zimmerman, Sliding crack model for nonlinearity and hysteresis in the uniaxial stress–strain curve of rock, Int. J. Rock. Mech. Min. Sci. 52 (2012) 9–17.

[138] F. Homand-Etienne, J.-P. Troalen, Behaviour of granites and limestones subjected to slow and homogeneous temperature changes, Eng. Geol. 20 (1984) 219–233.

[139] K. Kadoya, N. Matsunaga, A. Nagashima, Viscosity and thermal conductivity of dry air in the gaseous phase, J. Phys. Chem. Ref. Data 14 (1985) 947–970.

[140] A.E. Beck, Methods for determining thermal conductivity and thermal diffusivity, in: R. Haenel, L. Rybach, L. Stegena (Eds.), Handbook of Terrestrial Heat-Flow Density Determination, Kluwer Academic Publishers, Dordrecht, 1988.

[141] M.Y. Haller, C.A. Cruickshank, W. Streicher, S.J. Harrison, E. Andersen, S. Furbo, Methods to determine stratification efficiency of thermal energy storage processes—review and theoretical comparison, Sol. Energy 83 (10) (2009) 1847–1860.

[142] D.M. Crandall, E.F. Thacher, Segmented thermal storage, Sol. Energy 77 (2004) 435–440.

[143] H. Singh, R.P. Saini, J.S. Saini, Performance of a packed bed solar energy storage system having large sized elements with low void fraction, Sol. Energy 87 (2013) 22–34.

[144] Z. Wang, H. Wang, X. Li, D. Wang, Q. Zhang, G. Chen, Z. Ren, Aluminum and silicon based phase change materials for high capacity thermal energy storage, Appl. Therm. Eng. 89 (2015) 204–208.

[145] T. Sanderson, G. Cunningham, Performance and efficient design of packed bed thermal storage systems: part 1, Appl. Energy 50 (1995) 119–132.

[146] A. Saez, B. McCoy, Dynamic response of a packed bed thermal storage system-a model for solar air heating, Sol. Energy 29 (1982) 201–206.

[147] G. Zoth, R. Haenel, Thermal conductivity, in: R. Haenel, L. Rybach, L. Stegena (Eds.), Handbook of Terrestrial Heat Flow Density Determination, Kluwer Publishing, Dordrecht, 1988, pp. 449–468.

[148] H. Vosteen, Influence of temperature on thermal conductivity, thermal capacity and thermal diffusivity for different types of rock, Phys. Chem. Earth Parts A/B/C 28 (2003) 499–509.

[149] I. Kukkonen, A. Lindberg, Thermal properties of rocks at the investigation sites: measured and calculated thermal conductivity, specific heat capacity and thermal diffusivity, Working Report, 1998.

[150] A. Hartmann, V. Rath, C. Clauser, Thermal conductivity from core and well log data, Int. J. Rock. Mech. Min. Sci. 42 (2005) 1042–1055.

[151] U. Seipold, Temperature dependence of thermal transport properties of crystalline rocks – a general law, Tectonophys 291 (1998) 161–171.

[152] K. Horai, Thermal conductivity of rock-forming minerals, J. Geophys. Res. 76 (1971) 1278–1308.

[153] A. Jõeleht, I.T. Kukkonen, Thermal properties of granulite facies rocks in the Precambrian basement of Finland and Estonia, Tectonophys 291 (1988) 195–203.

[154] T. Baumann, S. Zunft, Properties of granular materials as heat transfer and storage medium in CSP application, Sol. Energy Mater. Sol. Cells 143 (2015) 38–47.